

Herlach (1961) proposed the phase transitions to IV and V from the observed changes in the ferroelectric behaviour as the temperature was reduced. Marked variations of the observed resonance-line intensities in the nuclear quadrupole resonance and dielectric constant (hysteresis loop size and shape in the Sawyer & Tower method) measurements, with temperature decrease, were cited as evidence of the transitions, although no significant changes to the X-ray powder diffraction pattern were observed.

The sample used was presumed to be a single crystal, although it is well known (Náray-Szabó & Kálmán, 1961) that twinned crystals are almost invariably produced in growth. A twinned crystal, or one with large ferroelectric domains (the electric Barkhausen effect was observed), under time-varying external magnetic or electric fields could produce the observed (nuclear quadrupole resonance and dielectric constant)

variations, with the observed phenomena arising from temperature-induced changes at this scale, rather than at the atomic level.

The author thanks Dr A. W. Hewat (ILL) for his assistance during the data collection, the Science and Engineering Research Council (UK) for support, and the ILL for making all facilities available to him.

References

- BACON, G. E. (1975). *Neutron Diffraction*. Oxford: Clarendon Press.
 HERLACH, F. (1961). *Helv. Phys. Acta*, **34**, 305–330.
 HEWAT, A. W. (1973). UKAEA Research Group R-7350 (unpublished).
 LUCAS, B. W. (1984). *Acta Cryst.* **C40**, 1989–1992.
 NÁRAY-SZABÓ, I. & KÁLMÁN, A. (1961). *Acta Cryst.* **14**, 791–792.
 RIETVELD, H. M. (1969). *J. Appl. Cryst.* **2**, 65–71.
 SCHNEIDER, C. S. (1976). *Acta Cryst.* **A32**, 375–379.

Acta Cryst. (1985). **C41**, 1391–1394

Structure of the New Zeolite Theta-1 Determined from X-ray Powder Data

BY RONA M. HIGHCOCK, GLEN W. SMITH AND DERMOTT WOOD

BP Research Centre, Sunbury-on-Thames, Middlesex TW16 7LN, England

(Received 7 December 1984; accepted 10 June 1985)

Abstract. SiO_2 , $M_r = 60.1$, orthorhombic, $Cmc2_1$, $a = 13.836$ (3), $b = 17.415$ (4), $c = 5.042$ (1) Å, $U = 1215$ Å³, $Z = 24$, $D_x = 1.97$ g cm⁻³, $\text{Cu K}\alpha$, $\lambda = 1.5418$ Å, $\mu = 72$ cm⁻¹, $F(000) = 720$, $T = 293$ K, $R = 0.116$ for 213 reflections with $I > 2\sigma(I)$. The structure was determined by structure modelling based upon two-dimensional Fourier projections; the intensities of the multiple overlapping reflections were extracted from the powder pattern. Conventional 'single-crystal-type' refinement techniques were used. The Si–Si bond distances and the geometry of the SiO_4 tetrahedra were as expected. Theta-1 is the first reported unidimensional medium-pore high-silica zeolite and it represents a new, topologically distinct, structure type.

Introduction. Synthetic high-silica zeolites exhibit a combination of properties which make them unique both scientifically and commercially. Physicochemical and catalytic studies of the new zeolite theta-1 indicated (Barri, Smith, White & Young, 1984) properties typical of a high-silica zeolite: it was thermally stable,

shape-selective and had acidic properties. Their results also showed a bulk $\text{SiO}_2:\text{Al}_2\text{O}_3$ molar ratio of 60:1, and that the zeolite was microporous with slightly elliptical pores of approximately 6 Å diameter. The present crystallographic study was undertaken to determine the structure unequivocally. It is notoriously difficult to synthesize large (*i.e.* >100 µm) single crystals of high-silica zeolites. Theta-1 is no exception. The typical size of the largest capped needle prisms was 0.1×2 µm. Therefore, since conventional X-ray structural methods were not appropriate, X-ray powder data were collected and used to derive, and refine, a trial structure.

Experimental. Theta-1 crystals were grown from a gel system as described elsewhere (European patent No. 0057049; published European patent application No. 0104800). Data were collected using a 17 cm vertical diffractometer, graphite monochromator, proportional counter, divergence slits ($\frac{1}{4}^\circ$ used for 5–14° 2θ , $\frac{1}{2}^\circ$ for 11–29°, 1° for 22–51° and 2° for 42–140°), Soller slits, $\frac{1}{2}^\circ$ receiving slit, instrumental profile breadth 0.15° (2θ), back-loaded sample, step scan, 0.02° steps,

FWHM 0.31° (2θ) at 8.16° (2θ). Data with $2\theta \leq 90^\circ$ used for solution and refinement; range of hkl $0 \rightarrow 12$, $0 \rightarrow 15$, $0 \rightarrow 4$.

Selected-area electron diffraction patterns revealed (Barri *et al.*, 1984) approximate unit-cell parameters and possible space groups $Cmcm$, $C2cm$ or $Cmc2_1$. 28 accurately calibrated and measured low-angle reflections were used in a least-squares refinement (Lindqvist & Wengelin, 1967) to produce accurate cell parameters. Calibration standards were zeolite Y $4\text{--}28^\circ$ (2θ), CeO_2 $28\text{--}80^\circ$ (2θ); angular corrections by linear interpolation; lattice parameters of standards 24.715 and 5.4110 \AA . All measurements were repeated on second samples and the values averaged.

From structural considerations, $Cmc2_1$ was thought to be the most likely space group because the presence of a mirror plane perpendicular to c in the other two possible space groups would have imposed too great a restriction on the positions of both the Si and the O atoms. At a much later stage an attempt at refinement in $Cmcm$ gave unsatisfactory results. At the start of the structure solution procedure 11 strong indexed $hk0$ reflections were selected and their intensities were extracted from the powder pattern as peak heights, ignoring all contributions from overlapping reflections. The sign of the lowest-angle reflection, 110, was fixed to select the origin and the signs of the next 6 reflections were systematically varied and used to compute 2^6 Fourier projections. The sign combination of the two most promising maps, chosen by consideration of the expected signs of the 220 and 400 reflections, were used as new starting points to calculate a further set of 2^4 Fourier projections by permuting the signs of the remaining reflections. However, the expected feature of a channel in the structure was not readily apparent. So although it is well known that Σ_2 relationships are unreliable when only two-dimensional data are used a manual derivation of signs was undertaken. This resulted in 8 signs being determined and 3 still uncertain. A further 2^3 Fourier projections were computed. The most physically plausible of these projections, but which in retrospect was found to have two incorrect phases, was used as a basis for structure modelling. A suitable Si framework, consistent with the space group, was derived. Further modelling and calculations based upon the known geometry of the SiO_4 unit enabled the positions of the O atoms to be deduced. Throughout the subsequent refinement it was assumed that the structure was composed purely of Si and O (no Al), and that the channels were empty.

Structure factors, calculated from the trial structure, were used to extract intensities of the individual reflections from the powder diffraction pattern. Estimated standard deviations were assigned as the square root of the intensities; the very weak reflections were given an arbitrary low F_o value and an appropriate high $\sigma(F)$. After refinement to convergence, the data

were reassessed using the freshly calculated structure factors. A third appraisal was made of the 52 reflections with the worst agreement between F_o and F_c . Final full-matrix least-squares refinement $\{\sum w(F_o - |F_c|)^2\}$ minimized; $w = [\sigma^2(I) + (0.05F^2)^2]^{-1/2}$ resulted in $R = 0.116$, $wR = 0.132$, $S = 1.72$ for 213 reflections with $I > 2\sigma(I)$; 89 reflections were classified as unobserved. All atoms isotropic; in final cycle of refinement max. $\Delta/\sigma = 0.41$; $\Delta\rho$ in final difference Fourier map $\pm 0.8 \text{ e \AA}^{-3}$; atomic scattering factors and corrections for anomalous dispersion from *International Tables for X-ray Crystallography* (1974). Refinement using *SDP-Plus* (Frenz, 1983); general data processing, data reduction and plotting of diffraction traces performed using locally written programs.

Discussion. Atomic coordinates are given in Table 1,* bond lengths and interbond angles in Table 2. The schematic framework is shown, together with the atom numbering scheme, in Fig. 1.

There are four independent Si atoms which do not form a closed polyhedron, but lie in a chain (Fig. 1). The action of the symmetry operators on these atoms produces an Si framework which is composed of five- and six-membered rings which link to form channels parallel to c . There are two such 10- T -ring channels per unit cell and, as shown in Fig. 2, they are slightly elliptical in cross-section. The zigzag chains of edge-shared 5-5- T rings in the a direction are linked at intervals of $\frac{1}{2}a$ by 6- T rings across the c glide. Similar structural features, although with different specific topologies, are found in ferrierite, ZSM-5 and ZSM-11 (Meier & Olson, 1978). In contrast, the Si framework is also related to that of bikitaite (Meier & Olson, 1978), whose unit cell is almost exactly a quarter of that of theta-1 in the ab plane but with a nearly identical c axis. The 5- T rings, in bikitaite, form very similar chains to those in theta-1 except that the linkage between the chains is direct.

The refinement of the structure has been limited because a true estimation of the overlapping reflection intensities could not be made. However, there is no doubt that the reported structure is essentially correct since it is supported by direct evidence of the structural arrangement in the ab projection which has been obtained by high-resolution transmission electron microscopy (Barri *et al.*, 1984), and the IR, adsorption, framework-density and magic-angle spinning NMR data (Barri *et al.*, 1984) are consistent with the structure. Further confirmation of the structure is provided by the calculated diffraction pattern which is shown

* Lists of structure factors, the experimental diffraction data and the calculated diffraction data have been deposited with the British Library Lending Division as Supplementary Publication No. SUP 42294 (9 pp.). Copies may be obtained through The Executive Secretary, International Union of Crystallography, 5 Abbey Square, Chester CH1 2HU, England.

together with the experimental data in Fig. 3. There is good general agreement between these two traces. The peak at approximately 21.7° (2θ) in the experimental trace is due to a cristobalite impurity. This peak was confirmed as an impurity by its absence in traces from other samples of theta-1. Some of the mismatch that does occur may be attributed to the omission of scattering density which may be present in the channels, e.g. adsorbed water. In the very first electron density maps (and in the Fourier projections) there were peaks present in the channels but the method of extracting the structure amplitudes based only on the calculated

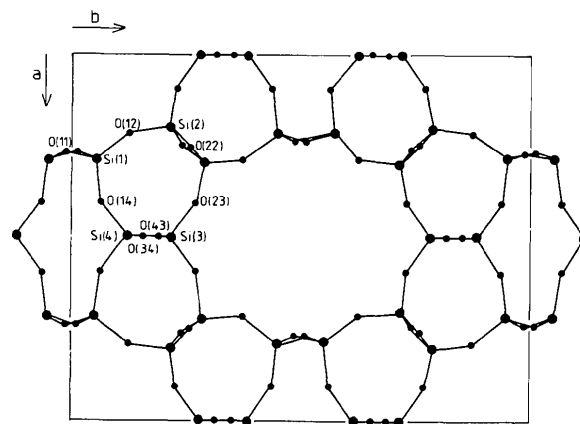


Fig. 1. Schematic drawing of the structure showing atom-labelling scheme.

Table 1. Fractional atomic coordinates and isotropic thermal parameters (\AA^2) with e.s.d.'s in parentheses

	<i>x</i>	<i>y</i>	<i>z</i>	<i>B</i>
Si(1)	0.2838 (9)	0.0503 (7)	0.250*	3.9 (3)
Si(2)	0.201 (1)	0.2157 (8)	0.312 (4)	4.9 (3)
Si(3)	0.500*	0.218 (1)	0.824 (6)	5.6 (5)
Si(4)	0.500*	0.118 (1)	0.320 (7)	7.3 (7)
O(11)	0.264 (2)	-0.010 (2)	0.493 (8)	6.2 (9)
O(12)	0.214 (2)	0.125 (2)	0.309 (8)	5.3 (8)
O(14)	0.404 (2)	0.065 (1)	0.280 (9)	4.9 (8)
O(22)	0.257 (3)	0.257 (2)	0.534 (7)	3.7 (7)
O(23)	0.407 (2)	0.269 (2)	0.795 (10)	6.7 (9)
O(34)	0.500*	0.152 (3)	0.628 (10)	6.2 (14)
O(43)	0.500*	0.187 (2)	1.132 (9)	4.3 (12)

* Fixed parameter.

Table 2. Bond lengths (\AA) and angles ($^\circ$) with e.s.d.'s in parentheses

Si(1)—Si(1 ¹)	3.070 (12)	Si(2)—O(12)	1.59 (2)
Si(1)—Si(2)	3.117 (14)	Si(2)—O(22)	1.54 (3)
Si(1)—Si(4)	3.237 (13)	Si(2)—O(22 ¹)	1.60 (3)
Si(2)—Si(2 ¹)	3.105 (12)	Si(2)—O(23 ¹)	1.52 (2)
Si(2)—Si(3 ¹)	3.006 (12)	Si(3)—O(23)	1.57 (2)
Si(3)—Si(4)	3.079 (43)	Si(3)—O(34)	1.51 (4)
Si(3)—Si(4 ¹)	3.047 (42)	Si(3)—O(43)	1.65 (4)
Si(1)—O(11)	1.64 (4)	Si(4)—O(14)	1.63 (2)
Si(1)—O(11 ¹)	1.50 (4)	Si(4)—O(34)	1.66 (5)
Si(1)—O(12)	1.65 (2)	Si(4)—O(43)	1.53 (4)
Si(1)—O(14)	1.70 (2)		
O(11)—Si(1)—O(11 ¹)	108.5 (8)	O(12)—Si(2)—O(22)	115 (2)
O(11)—Si(1)—O(12)	106 (2)	O(12)—Si(2)—O(22 ¹)	104 (2)
O(11)—Si(1)—O(14)	101 (2)	O(12)—Si(2)—O(23 ¹)	106 (1)
O(11 ¹)—Si(1)—O(12)	115 (2)	O(22)—Si(2)—O(22 ¹)	108.3 (7)
O(11 ¹)—Si(1)—O(14)	109 (2)	O(22)—Si(2)—O(23 ¹)	117 (2)
O(12)—Si(1)—O(14)	116 (1)	O(22 ¹)—Si(2)—O(23 ¹)	105 (2)
O(23)—Si(3)—O(23 ¹)	110 (2)	O(14)—Si(4)—O(14 ¹)	109 (2)
O(23)—Si(3)—O(34)	112 (2)	O(14)—Si(4)—O(34)	109 (2)
O(23)—Si(3)—O(43)	106 (2)	O(14)—Si(4)—O(43 ¹)	112 (2)
O(23 ¹)—Si(3)—O(34)	112 (2)	O(14 ¹)—Si(4)—O(34)	109 (2)
O(23 ¹)—Si(3)—O(43)	106 (2)	O(14 ¹)—Si(4)—O(43 ¹)	112 (2)
O(34)—Si(3)—O(43)	111 (2)	O(34)—Si(4)—O(43 ¹)	108 (2)
Si(1)—O(11)—Si(1 ¹)	156 (2)	Si(2 ¹)—O(23)—Si(3)	154 (2)
Si(1)—O(12)—Si(2)	148 (2)	Si(3)—O(34)—Si(4)	152 (3)
Si(1)—O(14)—Si(4)	154 (2)	Si(3)—O(43)—Si(4 ¹)	158 (3)
Si(2)—O(22)—Si(2 ¹)	165 (2)		

Symmetry codes

Si(1): (i) $x, -y, -\frac{1}{2} + z$

(ii) $x, -y, \frac{1}{2} + z$

Si(2): (i) $\frac{1}{2} - x, \frac{1}{2} - y, -\frac{1}{2} + z$

(ii) $\frac{1}{2} - x, \frac{1}{2} - y, \frac{1}{2} + z$

Si(3): (i) $\frac{1}{2} - x, \frac{1}{2} - y, -\frac{1}{2} + z$

Si(4): (i) $1 - x, y, 1 + z$

O(11): (i) $x, -y, -\frac{1}{2} + z$

O(14): (i) $1 - x, y, z$

O(22): (i) $\frac{1}{2} - x, \frac{1}{2} - y, -\frac{1}{2} + z$

O(23): (i) $\frac{1}{2} - x, \frac{1}{2} - y, -\frac{1}{2} + z$

(ii) $1 - x, y, z$

O(43): (i) $x, y, -1 + z$

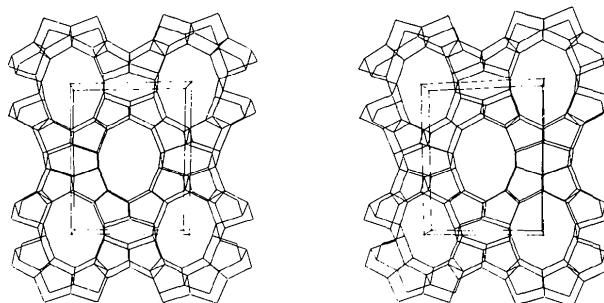


Fig. 2. ORTEP (Johnson, 1976) stereoview of the Si framework and channels viewed down *c* towards the origin which is at the top, back, right-hand corner.

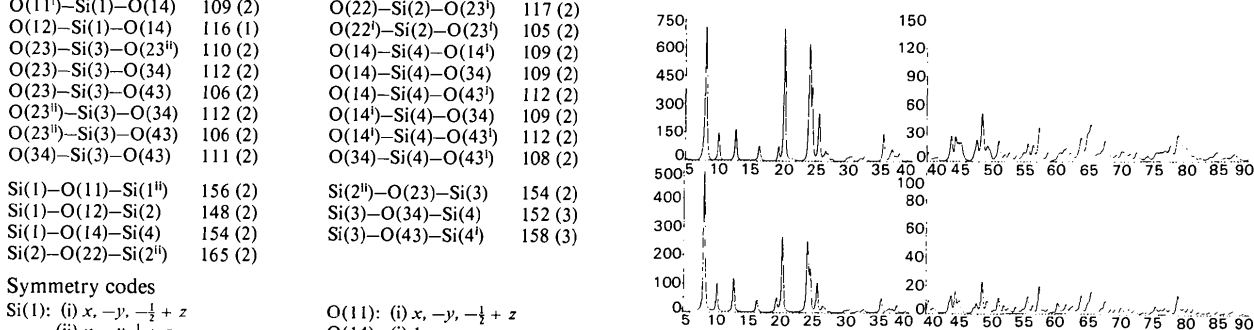


Fig. 3. Experimental (top) and calculated diffraction profiles of theta-1. Counts versus degrees 2θ . A 1:1 mixture of Gaussian and Lorentzian profiles was used for the calculated trace.

amplitudes of the Si—O framework resulted in these peaks being 'refined out'. A possible additional factor causing the mismatch may be residual preferred orientation in the sample, although great care was taken to eliminate it as far as possible. To establish the structural parameters of this novel zeolite with greater accuracy Rietveld analysis will be undertaken using X-ray data and neutron data, the latter in conjunction with Dr A. K. Cheetham (Oxford).

Theta-1 is the first reported example of the new, topologically distinct, structure type designated TON in accordance with IUPAC recommendations (Barrer, 1978). The unidimensional 10-*T*-ring channel system, unique for a high-silica zeolite, and the lack of channel intersections and associated 'cage' volumes (Derouane, 1980) should give theta-1 valuable structure-specific properties.

The authors thank Dr D. White for the electron diffraction studies, Dr S. A. I Barri for providing the

sample and BP International plc for permission to publish.

References

- BARRER, R. M. (1978). Chairman. *Chemical Nomenclature and Formulation of Compositions of Synthetic and Natural Zeolites*. Special IUPAC Commission booklet.
- BARRI, S. A. I., SMITH, G. W., WHITE, D. & YOUNG, D. (1984). *Nature (London)*, **316**, 533–534.
- DEROUANE, E. G. (1980). *Catalysis by Zeolites*, edited by B. IMELIK *et al.*, pp. 5–18. Amsterdam: Elsevier.
- FRENZ, B. A. (1983). *Enraf-Nonius Structure Determination Package; SDP Users Guide*, version January 1983.
- International Tables for X-ray Crystallography* (1974). Vol. IV. Birmingham: Kynoch Press. (Present distributor D. Reidel, Dordrecht.)
- JOHNSON, C. K. (1976). *ORTEP*. Report ORNL-5138. Oak Ridge National Laboratory, Tennessee.
- LINDQVIST, O. & WENGELIN, F. (1967). *Ark. Kemi*, **28**, 179–187.
- MEIER, W. M. & OLSON, D. H. (1978). *Atlas of Zeolite Structure Type*. Structure Commission of the International Zeolite Association.

Acta Cryst. (1985). **C41**, 1394–1396

Structure of Calcium Sodium Pentaborate

BY J. FAYOS, R. A. HOWIE AND F. P. GLASSER

Department of Chemistry, University of Aberdeen, Meston Walk, Old Aberdeen AB9 2UE, Scotland

(Received 15 April 1985; accepted 21 June 1985)

Abstract. CaNaB_5O_9 , $M_r = 261.1$, monoclinic, $P2_1/c$, $a = 6.463$ (5), $b = 13.932$ (11), $c = 7.858$ (6) Å, $\beta = 109.55$ (5)°, $V = 666.8$ Å³, $Z = 4$, $D_x = 2.601$ Mg m⁻³, $\lambda(\text{Mo } K\alpha) = 0.71069$ Å, $\mu = 1.009$ mm⁻¹, $F(000) = 512.0$, room temperature, final $R = 0.064$ for 594 unique observed reflections; crystal selected from synthetic material. The structure consists of complex metaborate sheets with a B_5O_9 building block. The B_5O_9 unit contains BO_4 and BO_3 groups in the ratio 2:3 in two rings. Na and Ca are partially ordered in sites in channels between the metaborate sheets.

Introduction. The preparation of CaNaB_5O_9 was first described in the course of investigations of the fluxing action of boric oxide in ceramic bodies (Mellor, 1980). Powder X-ray data reported for the phase are sufficient to equate it with the phase identified by Lawson (1981) as $\text{Na}_2\text{O} \cdot \text{CaO} \cdot 4\text{B}_2\text{O}_3$. Lawson studied phase relations in the system $\text{Na}_2\text{O} - \text{CaO} - \text{B}_2\text{O}_3$, and his liquidus phase equilibrium data disclosed compositional areas suitable for crystal growth of this phase from the melt. It melts incongruently, so crystals were grown from mixes

containing an excess of Na_2O and B_2O_3 . The melts were cooled very slowly: this, combined with some evaporation of Na_2O and B_2O_3 , enabled relatively large (*ca* 0.5 mm) crystals to be grown. The remaining melt persisted as glass and crystals were hand-picked under a petrographic microscope from the crushed mixture.

Experimental. Equant crystal ~0.2 mm diameter; Nicolet P3 diffractometer with Mo $K\alpha$ radiation and $\omega/2\theta$ scan method; cell refined from 14 reflections with $2\theta > 20^\circ$; no absorption correction applied; $\sin\theta/\lambda \leq 0.481$ Å⁻¹; indices in ranges $0 \leq h \leq 6$, $0 \leq k \leq 13$, $0 \leq |l| \leq 7$; no significant variation in intensities of standard reflections 161 and 014; 608 unique reflections, 14 classed as unobserved [$I < 2\sigma(I)$] and not used in any of the calculations. Structure solved using *MULTAN80* (Main *et al.*, 1980) and refined by block-diagonal least squares to minimize $\sum w(|F_o| - |F_c|)^2$ where w was calculated as $\{1 + [(|F_o| - 36)/17]^2\}^{-1}$. In refinement Ca and Na treated as vibrating anisotropically, O isotropically and B as fixed isotropic. $R = 0.064$, $wR = 0.070$. At end of refinement max. Δ/σ 0.07. Max. $\Delta\rho$ in final difference